

PAPER • OPEN ACCESS

The WENO reconstruction in the Godunov method for modeling hydrodynamic flows with shock waves

To cite this article: Kulikov Igor and Karavaev Dmitry 2021 *J. Phys.: Conf. Ser.* **2028** 012023

View the [article online](#) for updates and enhancements.

You may also like

- [DEPENDENCE OF THE SATURATION LEVEL OF MAGNETOROTATIONAL INSTABILITY ON GAS PRESSURE AND MAGNETIC PRANDTL NUMBER](#)
Takashi Minoshima, Shigenobu Hirose and Takayoshi Sano
- [RKDG method solution for hyperbolic hyperelastic model](#)
M V Alekseev, E B Savenkov and F N Voronin
- [Numerical experiments of flux difference splitting methods with high resolution scheme for supersonic flows](#)
Uttam Singh Rajput and Krishna Mohan Singh



The Electrochemical Society
Advancing solid state & electrochemical science & technology

241st ECS Meeting

May 29 – June 2, 2022 Vancouver • BC • Canada
Abstract submission deadline: Dec 3, 2021

Connect. Engage. Champion. Empower. Accelerate.
We move science forward



Submit your abstract



The WENO reconstruction in the Godunov method for modeling hydrodynamic flows with shock waves

Igor Kulikov and Dmitry Karavaev

Institute of Computational Mathematics and Mathematical Geophysics SB RAS,
6 Lavrentyev av., Novosibirsk, Russia

E-mail: kulikov@ssd.ssc.ru

Abstract. In the paper, we describe one simple WENO reconstruction for the Godunov method that allows one to get a version of the low-dissipation method. We describe in detail the procedure for reconstructing the "right" and "left" values of physical variables, which are used as arguments for an exact solution of the Riemann problem in the Godunov method. In the discontinuity decay test, we verify the quality of the developed numerical method and study its accuracy order. As a model task, the problem of multiple explosion of white dwarfs as a result of their high-speed collision in a three-dimensional problem statement will be considered.

1. Introduction

The Godunov method has been known for over 60 years and it is successfully used to solve hydrodynamic problems with discontinuous solutions and shock waves. After the original method had been developed many modifications of the Godunov method, aimed to reduce its numerical dissipation, have been proposed. The main modifications are MUSCL-like schemes [1, 2] and Kolgan solver [3], piecewise-parabolic method [4] and its compact implementation [5, 6] with extension to operator splitting approach [7], equations of magnetohydrodynamics [8] and relativistic hydrodynamics [9].

The main idea of all modifications is the use of piecewise polynomial representations of the solution. It brought with the development in the form of the WENO schemes [10, 11, 12, 13] with piecewise cubic representation of the solution [14, 15] up to the 17th order of precision [16]. Note that schemes like "Harten - Lax - van Leer" [17] or Lax-Wendroff [18] had been as the base solver. In this paper, we propose a new version of the modern implementation of the Godunov scheme [19] using the WENO reconstruction to obtain the low-dissipation property of the numerical method.

In the second section, we describe in detail the construction of the modern version of the Godunov method and the reconstruction of the solution to obtain the low-dissipation property. The third section deals with the verification of the numerical method on the Sod problem and the study of the convergence order of the developed method. The fourth section demonstrates the application of the developed numerical method to simulate multiple explosions of white dwarfs during their high-speed collision in the form of the Iax supernova explosion. The fifth section is a conclusion.



2. Numerical Method

Let us consider the equations of hydrodynamics in a one-dimensional case:

$$\begin{aligned}\frac{\partial \rho}{\partial t} + \frac{\partial (\rho u)}{\partial x} &= 0, \\ \frac{\partial \rho u}{\partial t} + \frac{\partial (\rho u^2 + p)}{\partial x} &= 0, \\ \frac{\partial}{\partial t} \left(\frac{p}{\gamma - 1} + \frac{\rho u^2}{2} \right) + \frac{\partial}{\partial x} \left(\left[\frac{p}{\gamma - 1} + \frac{\rho u^2}{2} + p \right] u \right) &= 0,\end{aligned}$$

where ρ is a density, u is a normal velocity, p is a pressure, γ is an adiabatic exponent, $c = \sqrt{\frac{\gamma p}{\rho}}$ is a sound speed.

In the computational domain, we introduce a uniform grid with a spatial step h . The time step τ is computed from the Courant condition:

$$\frac{\tau \times (c + \max |u|)}{h} = CFL < 1,$$

where CFL is Courant-Friedrichs-Lewy number. Also, to describe the numerical scheme, we introduce the value of the total mechanical energy:

$$\varepsilon = \frac{p}{\gamma - 1} + \frac{\rho u^2}{2}.$$

The values of conservative ($\rho, \rho u, \varepsilon$) and physical (ρ, u, p) variables are defined at the cell centers with a half-integer index. The values of flows through the boundaries of cells ($\rho u, \rho u^2 + p, [\varepsilon + p]u$) are defined at nodes with an integer index. The scheme of Godunov is written as:

$$\begin{aligned}\frac{\rho_{i+1/2}^{n+1} - \rho_{i+1/2}^n}{\tau} + \frac{R_{i+1}^n U_{i+1}^n - R_i^n U_i^n}{h} &= 0, \\ \frac{\rho u_{i+1/2}^{n+1} - \rho u_{i+1/2}^n}{\tau} + \frac{(R_{i+1}^n U_{i+1}^n U_{i+1}^n + P_{i+1}^n) - (R_i^n U_i^n U_i^n + P_i^n)}{h} &= 0, \\ \frac{\varepsilon_{i+1/2}^{n+1} - \varepsilon_{i+1/2}^n}{\tau} + \frac{\left(\frac{P_{i+1}^n}{\gamma - 1} + \frac{R_{i+1}^n U_{i+1}^n U_{i+1}^n}{2} + P_{i+1}^n \right) U_{i+1}^n - \left(\frac{P_i^n}{\gamma - 1} + \frac{R_i^n U_i^n U_i^n}{2} + P_i^n \right) U_i^n}{h} &= 0,\end{aligned}$$

where R_i^n, U_i^n, P_i^n is a solution of the discontinuity decay problem or the Riemann problem. Dirichlet-type conditions are used as boundary conditions.

Let us consider the solution of the linearized decay of the discontinuity for two neighboring cells (the index L denotes the left cell, the index R stands for the right cell) in accordance with the work [19]. In case of a supersonic flow on the left, when the condition $u_L > c_L$ is satisfied, the solution of the Riemann problem is:

$$P = p_L, \quad U = u_L, \quad R = \rho_L.$$

In the case of a supersonic flow on the right, that is, when the condition $u_R < -c_R$ is satisfied, the solution to the Riemann problem is:

$$P = p_R, \quad U = u_R, \quad R = \rho_R.$$

Otherwise, the velocity of the left wave is computed by the equation:

$$dx/dt = u_L - c_L,$$

and the following condition is satisfied on it:

$$(u_L - U) + \frac{p_L - P}{\rho_L c_L} = 0.$$

The speed of the right wave is computed by the formula:

$$dx/dt = u_R + c_R,$$

and there is the next condition on it:

$$(u_R - U) - \frac{p_R - P}{\rho_R c_R} = 0.$$

As a result, the values of the velocity U and pressure P at the boundary of the cells are computed by the equations:

$$P = \frac{\frac{p_L}{\rho_L c_L} + \frac{p_R}{\rho_R c_R} + u_L - u_R}{\frac{1}{\rho_L c_L} + \frac{1}{\rho_R c_R}},$$

$$U = \frac{\rho_L c_L u_L + \rho_R c_R u_R + p_L - p_R}{\rho_L c_L + \rho_R c_R}.$$

In the paper [19] there had been proposed the original approach based on the constant value of $p - \rho c^2$ at the characteristics $dx/dt = u \pm c$:

$$P - Rc_R^2 = p_R - \rho_R c_R^2, \quad P - Rc_L^2 = p_L - \rho_L c_L^2.$$

As a result, the sign of the velocity U depends on the solution for the density R at the boundary of the cells, calculated by the equation:

$$R = \begin{cases} \rho_L \left(1 - \frac{U - u_L}{c_L}\right), & U \geq 0 \\ \rho_R \left(1 - \frac{u_R - U}{c_R}\right), & U < 0 \end{cases}.$$

Using the above formulas, fluxes across the boundary of the corresponding physical variables are computed in the Godunov method.

For WENO, the reconstructions of the physical variables ρ , u and p (denoted by the function f) on the interface i are computed by the following equations:

$$f_L^{WENO} = \omega_{L,1} f_{L,1} + \omega_{L,2} f_{L,2} + \omega_{L,3} f_{L,3}, \quad f_R^{WENO} = \omega_{R,1} f_{R,1} + \omega_{R,2} f_{R,2} + \omega_{R,3} f_{R,3},$$

where

$$f_{L,1} = \frac{11}{6} f_{i-\frac{1}{2}} - \frac{7}{6} f_{i-\frac{3}{2}} + \frac{2}{6} f_{i-\frac{5}{2}},$$

$$f_{L,2} = \frac{2}{6} f_{i+\frac{1}{2}} + \frac{5}{6} f_{i-\frac{1}{2}} - \frac{1}{6} f_{i-\frac{3}{2}},$$

$$f_{L,3} = -\frac{1}{6} f_{i+\frac{3}{2}} + \frac{5}{6} f_{i+\frac{1}{2}} + \frac{2}{6} f_{i-\frac{1}{2}},$$

$$f_{R,1} = \frac{11}{6} f_{i+\frac{1}{2}} - \frac{7}{6} f_{i+\frac{3}{2}} + \frac{2}{6} f_{i+\frac{5}{2}},$$

$$f_{R,2} = \frac{2}{6}f_{i-\frac{1}{2}} + \frac{5}{6}f_{i+\frac{1}{2}} - \frac{1}{6}f_{i+\frac{3}{2}},$$

$$f_{R,3} = -\frac{1}{6}f_{i-\frac{3}{2}} + \frac{5}{6}f_{i-\frac{1}{2}} + \frac{2}{6}f_{i+\frac{1}{2}}.$$

To compute the coefficients $\omega_{L,i}$ and $\omega_{R,i}$, the following equations are used:

$$\omega_{L,i} = \frac{\sigma_{L,i}}{\sigma_{L,1} + \sigma_{L,2} + \sigma_{L,3}}, \quad \omega_{R,i} = \frac{\sigma_{R,i}}{\sigma_{R,1} + \sigma_{R,2} + \sigma_{R,3}},$$

where $\sigma_{L,i}$ and $\sigma_{R,i}$ are calculated as:

$$\sigma_{L,1} = \frac{1}{10(\epsilon + \beta_{L,1})^5}, \quad \sigma_{L,2} = \frac{6}{10(\epsilon + \beta_{L,2})^5}, \quad \sigma_{L,3} = \frac{3}{10(\epsilon + \beta_{L,3})^5},$$

$$\sigma_{R,1} = \frac{1}{10(\epsilon + \beta_{R,1})^5}, \quad \sigma_{R,2} = \frac{6}{10(\epsilon + \beta_{R,2})^5}, \quad \sigma_{R,3} = \frac{3}{10(\epsilon + \beta_{R,3})^5},$$

where $\epsilon = 10^{-36}$ has been used. Values of $\beta_{L,i}$ and $\beta_{R,i}$ are computed by the equations:

$$\beta_{L,1} = \frac{13}{12} \left(f_{i-\frac{5}{2}} - 2f_{i-\frac{3}{2}} + f_{i-\frac{1}{2}} \right)^2 + \frac{1}{4} \left(f_{i-\frac{5}{2}} - 4f_{i-\frac{3}{2}} + 3f_{i-\frac{1}{2}} \right)^2,$$

$$\beta_{L,2} = \frac{13}{12} \left(f_{i-\frac{3}{2}} - 2f_{i-\frac{1}{2}} + f_{i+\frac{1}{2}} \right)^2 + \frac{1}{4} \left(f_{i-\frac{3}{2}} - f_{i+\frac{1}{2}} \right)^2,$$

$$\beta_{L,3} = \frac{13}{12} \left(f_{i-\frac{1}{2}} - 2f_{i+\frac{1}{2}} + f_{i+\frac{3}{2}} \right)^2 + \frac{1}{4} \left(3f_{i-\frac{1}{2}} - 4f_{i+\frac{1}{2}} + f_{i+\frac{3}{2}} \right)^2,$$

$$\beta_{R,1} = \frac{13}{12} \left(f_{i+\frac{5}{2}} - 2f_{i+\frac{3}{2}} + f_{i+\frac{1}{2}} \right)^2 + \frac{1}{4} \left(f_{i+\frac{5}{2}} - 4f_{i+\frac{3}{2}} + 3f_{i+\frac{1}{2}} \right)^2,$$

$$\beta_{R,2} = \frac{13}{12} \left(f_{i+\frac{3}{2}} - 2f_{i+\frac{1}{2}} + f_{i-\frac{1}{2}} \right)^2 + \frac{1}{4} \left(f_{i+\frac{3}{2}} - f_{i-\frac{1}{2}} \right)^2,$$

$$\beta_{R,3} = \frac{13}{12} \left(f_{i+\frac{1}{2}} - 2f_{i-\frac{1}{2}} + f_{i-\frac{3}{2}} \right)^2 + \frac{1}{4} \left(3f_{i+\frac{1}{2}} - 4f_{i-\frac{1}{2}} + f_{i-\frac{3}{2}} \right)^2.$$

After the WENO reconstruction, we solve the Riemann problem for the values:

$$f^L = \frac{3}{10}f_L + \frac{7}{10}f_L^{WENO}, \quad f^R = \frac{3}{10}f_R + \frac{7}{10}f_R^{WENO}.$$

Note that the choice of some coefficients was based on computational experiments.

3. Verification

Consider the Sod problem for ideal gas with $\gamma = 1.4$ in the interval $[0; 1]$ up to the time $t = 0.2$. Gas is static $u = 0$ at the initial time. We choose the following statement of the problem: to the left of the discontinuity at $x_0 = 0.5$ the pressure is $p_L = 2$ and the density is $\rho_L = 2$, to the right of the discontinuity there are $p_R = 1$ and $\rho_R = 1$. For all the experiments presented in the paper, there are used the Courant number $CFL = 0.2$ and $N = 100$ (the number of cells in the computational domain). The results of the computational experiments using the Godunov method are presented in the figure (1). Note that when using the low-dissipation variant of the Godunov scheme, it is possible to reduce the dissipation on the shock wave from nine to one cell.

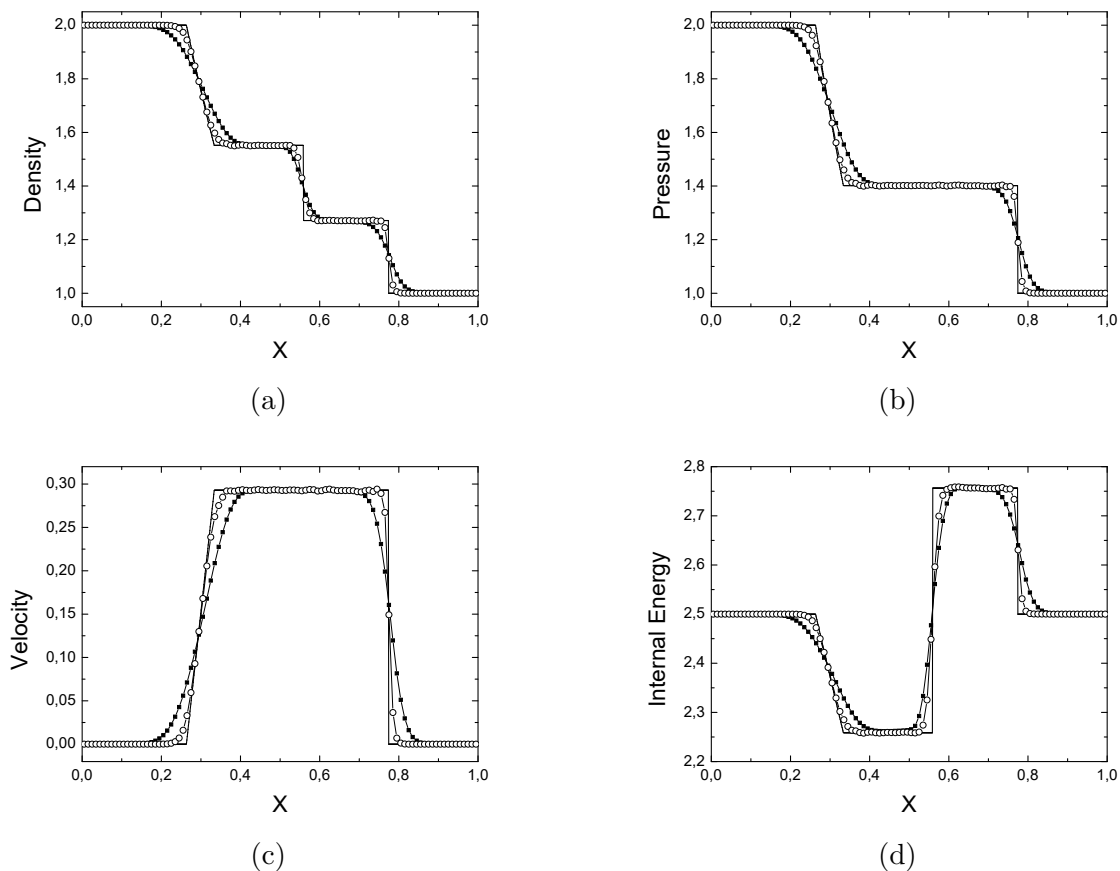


Figure 1. Numerical solution when using original scheme (squares), low-dissipation scheme (circles) and exact solution (solid line) for density (a), pressure (b), velocity (c) and internal energy (d).

To estimate the convergence of this method, we study the behavior of the L_1 norm errors:

$$L_1 = \sum_i h |u_i - u(x_i)|,$$

where $u(x_i)$ is the exact solution at x_i , u_i is the numerical result, and h is spacing of an uniform grid. The behavior of the L_1 norm for the Sod problem can be seen from the table (1). From the table (1) it can be seen that the convergence for the density function drops almost to its half value, then increases and becomes of the convergence order of ~ 0.6 . For pressure and velocity functions, the behavior of the convergence order is similar. Such behavior of the convergence order for a discontinuous solution took place for the classical Godunov scheme, also.

4. Astrophysics Simulation

As a model astrophysical problem, let us consider the multiple explosion of white dwarfs of the solar mass as a result of their high-speed collision in the three-dimensional formulation [20]. The mathematical model of the evolution of white dwarfs is based on solving the overdetermined system of gravitational hydrodynamics [21]. To close the gravitational hydrodynamics, the adaptation of the stellar equation of state [22] is used. It consists of the contribution of the pressure of a nondegenerate hot gas, pressure due to radiation and a degenerate gas. In the case

Primitive variables	Mesh	L_1 error	Convergence Rate
Density	100	6.91e-03	
	200	4.16e-03	0.73
	400	2.98e-03	0.48
	800	2.07e-03	0.53
	1600	1.36e-03	0.61
	3200	8.81e-04	0.62
Pressure	100	5.69e-03	
	200	3.18e-03	0.84
	400	2.38e-03	0.42
	800	1.77e-03	0.43
	1600	1.18e-03	0.58
	3200	7.88e-04	0.59
Velocity	100	3.65e-03	
	200	1.87e-03	0.97
	400	1.32e-03	0.49
	800	9.39e-04	0.51
	1600	6.15e-04	0.61
	3200	4.12e-04	0.58

Table 1. L_1 errors for the Sod test.

of a degenerate gas, the relativistic and nonrelativistic regimes are considered. As a net of nuclear systems, we consider the α -network [23]. In the computational experiment, the temperature of the dwarfs reached the value of $T = 10^8$ K. At the distance of 200 km from the point of explosion, many satellite bubbles had appeared. The figure (2) shows the density isosurface at the time of $t = 5$ seconds. It can be seen from the figure (2) that the combustion fronts are correctly

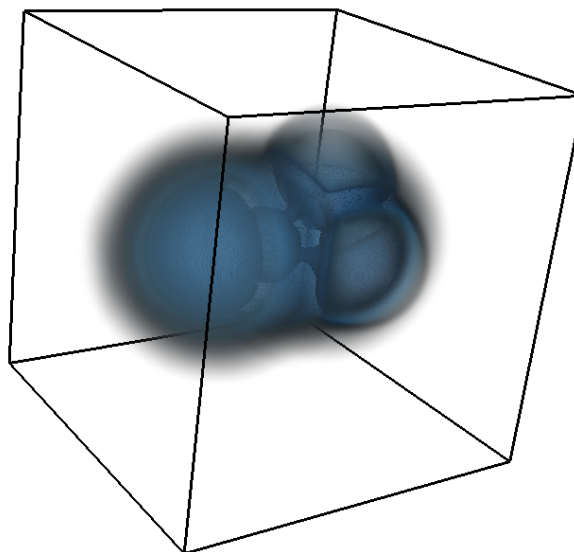


Figure 2. The density of the supernova Iax type simulation.

reproduced due to the subsonic turbulent combustion of carbon. These results confirm the conclusions that ignition and transition to the detonation combustion are not required to obtain sufficiently powerful explosions. In the mathematical model, we use the ultimate adiabatic model of the state equation for a degenerate gas, which limits our possibilities for a more realistic account of the physics of the explosion in terms of chemical composition. However, the state equation applied in this work and allowing to describe enough the hydrodynamics of the evolution of white dwarfs and the supernova explosions is also widely used.

5. Conclusion

A simple low-dissipation WENO reconstruction of the Godunov scheme has been proposed. In the paper there has been described in detail the procedure for reconstructing the "right" and "left" values of physical variables, which are used as arguments for the exact solution of the Riemann problem in the Godunov method. The numerical method has been verified on the Sod problem both in terms of the solution quality and accuracy order of the scheme. The supernova explosion of Iax type based on a high-speed collision of white dwarfs has been used as an astrophysical application to verify the numerical method.

Acknowledgements

This work was supported by the Russian Science Foundation (project 18-11-00044) <https://rscf.ru/project/18-11-00044/>.

References

- [1] Van Leer B. Towards the Ultimate Conservative Difference Scheme, V. A Second Order Sequel to Godunov's Method // *Journal of Computational Physics*. – 1979. – V. 32. – P. 101-136.
- [2] Kurganov A., Tadmor E. New High-Resolution Central Schemes for Nonlinear Conservation Laws and Convection-Diffusion Equation // *Journal of Computational Physics*. – 2000. – V. 160. – P. 214-282.
- [3] Tunik Yu.V. Numerical Solution of Test Problems Using a Modified Godunov Scheme // *Computational Mathematics and Mathematical Physics*. – 2018. – V. 58. – P. 1573-1584.
- [4] Collella P., Woodward P.R. The Piecewise Parabolic Method (PPM) Gas-Dynamical simulations // *Journal of Computational Physics*. – 1984. – V. 54. – P. 174-201.
- [5] Popov M., Ustyugov S. Piecewise parabolic method on local stencil for gasdynamic simulations // *Computational Mathematics and Mathematical Physics*. – 2007. – V. 47, I. 12. – P. 1970-1989.
- [6] Kulikov I., Chernykh I., Tutukov A. A New Hydrodynamic Code with Explicit Vectorization Instructions Optimizations that Is Dedicated to the Numerical Simulation of Astrophysical Gas Flow. I. Numerical Method, Tests, and Model Problems // *The Astrophysical Journal Supplement Series*. – 2019. – V. 243. – Article Number 4.
- [7] Kulikov I., Vorobyov E. Using the PPML approach for constructing a low-dissipation, operator-splitting scheme for numerical simulations of hydrodynamic flows // *Journal of Computational Physics*. – 2016. – V. 317. – P. 318-346.
- [8] Popov M., Ustyugov S. Piecewise parabolic method on a local stencil for ideal magnetohydrodynamics // *Computational Mathematics and Mathematical Physics*. – 2008. – V. 48, I. 3. – P. 477-499.
- [9] Kulikov I. A new code for the numerical simulation of relativistic flows on supercomputers by means of a low-dissipation scheme // *Computer Physics Communications*. – 2020. – V. 257. – Article Number 107532.
- [10] Jiang G.-S., Shu C.-W. Efficient Implementation of Weighted ENO Schemes // *Journal of Computational Physics*. – 1996. – V. 126. – P. 202-228.
- [11] Balsara D., Shu C.-W. Monotonicity Preserving Weighted Essentially Non-oscillatory Schemes with Increasingly High Order of Accuracy // *Journal of Computational Physics*. – 2000. – V. 160. – P. 405-452.
- [12] Henrick A., Aslam T., Powers J. Mapped weighted essentially non-oscillatory schemes: Achieving optimal order near critical points // *Journal of Computational Physics*. – 2005. – V. 207. – P. 542-567.
- [13] Balsara D., Rumpf T., Dumbser M., Munz C.-D. Efficient, high accuracy ADER-WENO schemes for hydrodynamics and divergence-free magnetohydrodynamics // *Journal of Computational Physics*. – 2009. – V. 228. – P. 2480-2516.
- [14] Titarev V.A., Toro E.F. ADER schemes for three-dimensional nonlinear hyperbolic systems // *Journal of Computational Physics*. – 2005. – V. 204. – P. 715-736.

- [15] Lee D., Faller H., Reyes A. The Piecewise Cubic Method (PCM) for computational fluid dynamics // *Journal of Computational Physics*. – 2017. – V. 341. – P. 230-257.
- [16] Gerolymos G.A., Senechal D., Vallet I. Very-high-order WENO schemes // *Journal of Computational Physics*. – 2009. – V. 228. – P. 8481-8524.
- [17] Liu H. A numerical study of the performance of alternative weighted ENO methods based on various numerical fluxes for conservation law // *Applied Mathematics and Computation*. – 2017. – V. 296. – P. 182-197.
- [18] Dong H., Lu C., Yang H. The Finite Volume WENO with Lax-Wendroff Scheme for Nonlinear System of Euler Equations // *Mathematics*. – 2018. – V. 6. – Article Number 211.
- [19] Godunov S.K., Klyuchinskii D.V., Fortova S.V., Shepelev V.V. Experimental Studies of Difference Gas Dynamics Models with Shock Waves // *Computational Mathematics and Mathematical Physics*. – 2018. – V. 58. – P. 1201-1216.
- [20] Reinecke M., Hillebrandt W., Niemeyer J.C. Three-dimensional simulations of type Ia supernovae // *Astronomy & Astrophysics*. – 2002. – V. 391. – P. 1167-1172.
- [21] Kulikov I.M., Chernykh I.G., Sapetina A.F., Lomakin S.V., Tutukov A.V. A New Rusanov-Type Solver with a Local Linear Solution Reconstruction for Numerical Modeling of White Dwarf Mergers by Means Massive Parallel Supercomputers // *Lobachevskii Journal of Mathematics*. – 2020. – V. 41. – P. 1485-1491.
- [22] Timmes F.X., Arnett D. The accuracy, consistency, and speed of five equations of state for stellar hydrodynamics // *The Astrophysical Journal Supplement Series*. – 1999. – V. 125. – P. 277-294.
- [23] Steinmetz M., Muller E., Hillebrandt W. Carbon Detonations in Rapidly Rotating White Dwarfs // *Astronomy & Astrophysics*. – 1992. – V. 254. – P. 177-190.